Permittivity and Permeability of Polycrystalline Ba(CoZr)xFe12–2xO19 and Their Composite Thick Films at RF and Microwave Frequencies

Mukesh C. Dimri[1]*, D. C. Dube[2]

[1] Jaypee University Anoopshahr, Anoopshahr-203390, Bulandshahr, India
[2] Department of EECE, ITM University, Gurgaon 122017, India

*Communicating author: Tel. +918800420903; email: mukeshdimri@yahoo.com
Manuscript submitted April 28, 2015; accepted September 11, 2015.
doi: 10.17706/ijmse.2015.3.3.208-218

Abstract: In this paper the effect of Co-Zr substitution on permittivity and permeability of polycrystalline M-type hexaferrite ($Ba(CoZr)_xFe_{12-2x}O_{19}$ with $0 \le x \le 0.5$) and their composite thick films was investigated at RF and microwave frequencies (X- band). Enhanced sintering temperatures as well as higher Co-Zr concentration in the polycrystalline $Ba(CoZr)_xFe_{12-2x}O_{19}$ samples resulted in enhancement in the complex permittivity. This rise in permittivity is understandable in ferrites due to increased concentration of easily polarizable Fe^{2+} ions in the high temperature sintered samples. Co-Zr substitution resulted in grain growth, enhancement in electrical conductivity and enhanced dielectric parameters. Permeability of these samples, measured at X-band frequencies by cavity perturbation technique, was found to be decreasing on Co-Zr substitution, because of substitution of magnetic Fe ions by nonmagnetic Zr ions. However the complex permittivity don't show remarkable change within X-band frequency range. The permittivity values of thick films were expectedly found to be less as compared to corresponding bulk materials both at low and microwave frequencies. Temperature dependence of dielectric properties of these ferrite-composite thick films also infers that these films can be useful up to a temperature of 200°C without material degradation.

Key Words: M-type hexaferrites, complex permittivity and permeability, composite thick films

1. Introduction

Pure and substituted M-type barium hexaferrites ($BaFe_{12}O_{19}$) have been intensively investigated due to their application in a variety of magnetic and electronic devices such as high density magneto-optical recording, microwave devices and components, ferrite cores, filler in the magnetocomposites and recently as multiferroics [1–8]. Greater permeability, high Curie temperature and higher magnetic resonance frequency of hexaferrites than spinel ferrites make these materials and their composites suitable for microwave absorbers in the GHz range [9, 10]. $BaFe_{12}O_{19}$ has strong magnetocrystalline anisotropy along c-axis, this strong uniaxial anisotropy leads to low permeability and high resonant frequency (f = 42.5GHz) [11]. It is well known that the dielectric and magnetic properties can be modulated by substitution for Fe^{3+} and Ba^{2+} ions with suitable dopant ions. Different cations or cation combinations such as Zn-Ti, Sn–Ru, Co–Ti, Co–Ir, Zn–Ir, Ni–Sn, (Co,Zn)–Ru, Mn, and Cu–Ti have been used to partially substitute Fe^{3+} in barium hexaferrite to reduce its high magnetic uniaxial anisotropy without much affecting the saturation magnetization (Ms) for applications in high-density magnetic recording and microwave absorption devices [12-18]. Choosing an

appropriate synthesis route, optimizing the synthesis conditions and suitable dopants have been used to modify the magnetic and dielectric properties [19-24]. The values of complex relative permittivity and permeability of constituent material of a microwave absorber determine the reflection and attenuation characteristics of the absorber. It is, therefore, important to study these properties at microwave frequencies. There are very few studies on complex permittivity and permeability of Co-Zr substituted barium hexaferrite bulk samples [25], and no studies on their composite thick films in the GHz region. Though, we had earlier reported the dielectric and magnetic properties of Co-Zr doped barium hexaferrite nanopowders and their composites in our previous study [26].

Due to lack of literature on microwave measurements on bulk and polymer composites thick films of $Ba(CoZr)_xFe_{12-2x}O_{19}$ (x = 0, 0.1, 0.2, 0.35 and 0.5) hexaferrites, a systematic study have been done. The dopant concentration above x = 0.5 resulted in the segregation of secondary phases, so the present study was limited below this dopant level. The effects of dopants and sintering temperature on permittivity and permeability at RF as well as at microwave frequencies have been investigated and reported in this article.

2. Experimental

Polycrystalline bulk samples of $Ba(CoZr)_xFe_{12-2x}O_{19}$ (x = 0, 0.1, 0.2, 0.35 and 0.5) were prepared by citrate precursor method. Analytical grade metal nitrates and acetates were used as the starting materials. A stoichiometric amount of aqueous solutions of $Ba(NO_3)_2$, $Fe(NO_3).9H_2O$, $Co(NO_3)_3.6H_2O$ and zirconium acetate was dissolved in citric acid solution under constant stirring. The molar ratio of cations to citric acid was 1:1. Then, an appropriate amount of ammonia solution was dropped into the solution under continuous stirring to adjust the pH value to around 7. The mixed precursor solution was heated at 80°C under continuous stirring till the solvent is completely evaporated off. Further heating of 80°C completes the combustion process and results into a fluffy powder. That powder is calcined at 600°C for 1 hour, and later disc shape uniaxially pressed pellets were sintered at 1200°C for 3 hours. Besides, an undoped sample was sintered at various temperatures in the range 1100-1300°C for 3 hours. Composite thick films of $Ba(CoZr)_xFe_{12-2x}O_{19}$ - polymer were prepared by mixing the ferrite powder with an epoxy resin (EPG280) in different weight ratios, and the paste like mixture was molded in the shape of sheets (of thicknesses below 100 micrometers) .

Powder X-ray diffraction patterns of the polycrystalline samples were recorded (Rigaku X-ray diffractometer, source Cu Kα) for ascertaining the single phase formation and grain size. SEM micrographs (using Cambridge stereoscan 360 scanning electron microscope) were employed to determine the microstructure and particle size. For the dielectric measurements the disk shape pellets and composite films were coated with silver electrodes. Frequency (50 Hz–1 MHz) and temperature dependence of dielectric constant and dielectric loss were recorded with the help of precision LCR meter (Hewlett Packard model 4284A). A cavity perturbation technique [26] was used to determine the complex permittivity and permeability at X-band microwave frequencies (8 – 12 GHz) using a vector network analyzer (model HP8719ES). These parameters are calculated at specific frequencies due to limited electric and magnetic resonant modes in cavity. The details about the cavity and method of measuring complex permittivity and permeability have been described in earlier publications [26, 27].

3. Results and Discussions

3.1. Structure

X-ray diffractograms for the polycrystalline $Ba(CoZr)_xFe_{12-2x}O_{19}$ samples are shown in Fig. 1. Comparison with standard data (JSPDS file # 84757) reveals single phase hexaferrite formation for all the compositions. The dopant concentration (Co-Zr) above x = 0.5 resulted in the segregation of impurity phases (so higher

concentrations are not included for further studies). Lattice parameters are given in Table 1. It may be noted from the table that the lattice parameter 'a' increases slightly, whereas the lattice parameter 'c' decreases with increase in the Co and Zr concentration. This may be due to the difference in ionic radii of Co^{2+} (0.65 Å) and Zr^{4+} (0.72 Å) ions as compared to the octahedral iron (Fe^{3+}) ions (0.55 Å) [28]. The 'c/a' ratio, therefore, decreases with the increase in the concentration of substituent ions. It indicates that change of easily magnetized c-axis is larger than a-axis with Co^{2+} and Zr^{4+} ions substitution. Co^{2+} cations prefer to occupy the octahedral iron sites ($4f_2$ and 2b), whereas Zr^{4+} ions prefer tetrahedral ($4f_2$) and trigonal bipyramidal ($4f_1$) lattice sites [29, 30]. However, the c/a ratio have been reported to increase in $Ba(CoZr)_xFe_{12-2x}O_{19}$ samples prepared by conventional ceramic route [25]. The contrary behavior in our samples may be due to difference in synthesis method (chemical solution method) and presence of oxygen vacancies during sintering. The sintering at higher temperature changes the iron valence Fe^{3+} to Fe^{2+}, those have larger ionic radii (0.78 Å) as compared to Co^{2+} and Zr^{4+} ions. The grain (crystallite) sizes were also calculated using the Debye – Scherrer's formula [31] and were found to be nearly 25 nm.

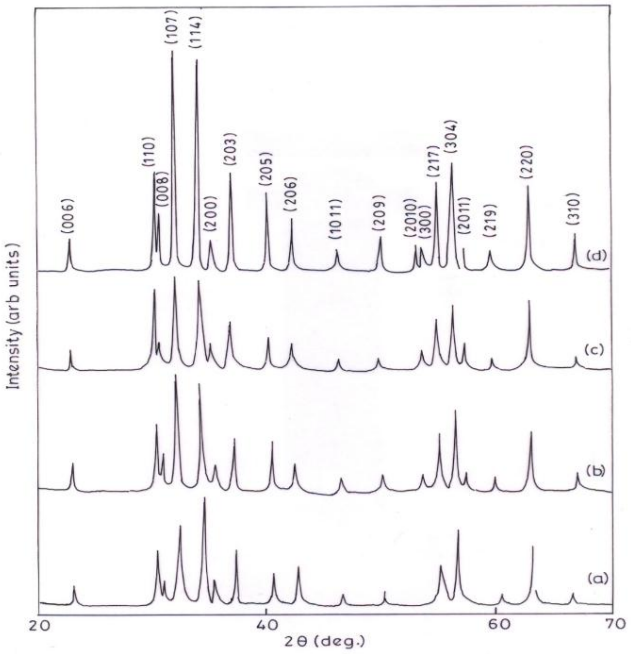

Fig. 1. X-ray diffractograms of polycrystalline Ba(CoZr)xFe12-2xO19 samples sintered at 1200°C for 3 hours (a) x = 0.5, (b) x = 0.35 (c) x = 0.2 and (d) x = 0.0.

Table 1. Lattice Parameters (with Estimated Errors), Grain Sizes and Particle Size of the Polycrystalline Ba(CoZr)xFe12-2xO19 Bulk Samples

Composition (x)	'a' (Å) (± 1%)	'c' (Å) (± 1%)	c/a ratio	Approximate particle size (μm)	Crystallite size from XRD (nm)
0.00	5.89	23.26	3.95	4	32
0.20	5.90	23.22	3.94	3	22
0.35	5.90	23.14	3.92	9	27
0.50	5.91	23.01	3.89	7	25

3.2. Frequency Dependence of Dielectric Properties of Pristine and Doped Samples

3.2.1 Pristine barium hexaferrite samples

Before preparing cation substituted samples, an effort was made to fabricate pristine samples with good dielectric properties over the radiofrequency range, by carrying out solid state sintering at three different temperatures. The dielectric constant (ε′) and loss factor (tanδ= ε′′/ε′) estimated at RF frequencies (50 Hz - 1 MHz) for undoped barium hexaferrite samples sintered at 1100, 1200 and 1300°C are plotted in the Fig. 2. The Dielectric constant of the sample sintered at 1200°C is higher than the corresponding values for the sample sintered at 1100°C, and is almost unchanged over the entire range (except at lower frequencies, where the values are higher) unlike the sample sintered at 1300°C (which shows much higher values at lower frequencies). It may be noted that the sample prepared at 1300°C exhibits much higher loss values over the entire frequency range, and also records unusual increase in the loss tangent with frequency, though the trend starts showing up in the other samples too. Thus the sample sintered at 1200°C is most suitable for further studies by after doping.

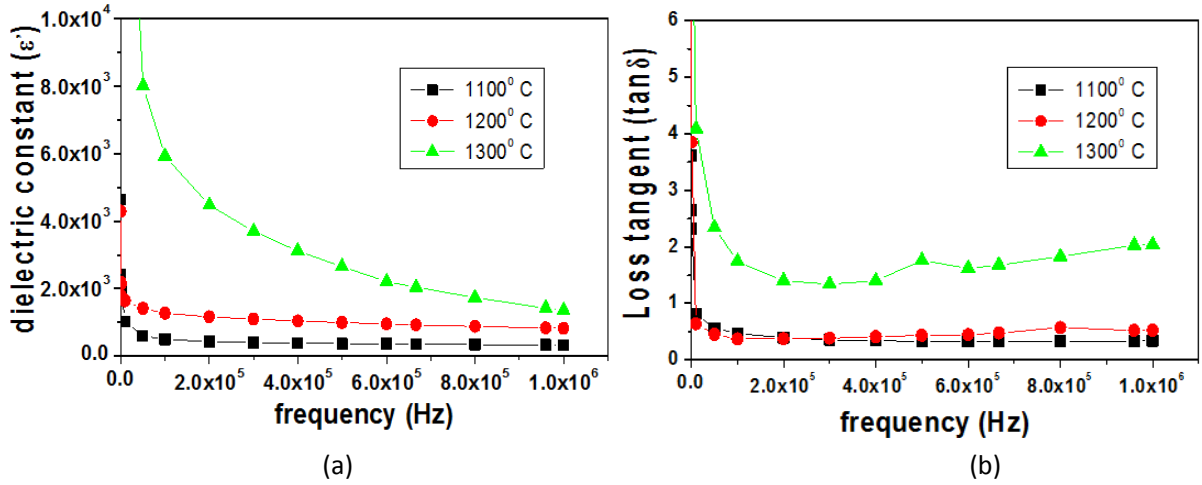

Fig. 2. Frequency dependence of (a) The dielectric constant and (b) Loss tangent for the polycrystalline barium hexaferrite (BaFe12O19) samples sintered at different temperatures.

Variation of the real and imaginary parts of the permittivity with the X-band frequencies is shown in Fig. 3. The properties of the samples are almost unchanged in this frequency range. The values of dielectric parameter (ε′) are higher for the ferrites sintered at higher temperatures, as it was also observed at lower frequencies, and increase monotonically with frequency except that the maximum value is obtained for the sample sintered at 1200°C. Dielectric constant is increased two fold at this sintering temperature. The dielectric losses also rises in general for samples sintered at higher temperatures. However, the sample sintered at 1200°C shows less variation than the one sintered at 1300°C. Almost unchanged values of dielectric parameter (ε′) both in the RF and microwave range, and its maximum value in the MW range with least variation in tan δ for the sample sintered at 1200°C , make it an optimum temperature for sintering.

The observed increase in the dielectric parameters with sintering temperature can be understood by considering the variation in electrical conductivity with sintering temperature. Sintering at higher temperature enhances the Fe^{2+} ions, which are more conducting ions as compared to other cations present in ferrites. Presence of more Fe^{2+} ions due to sintering at higher temperatures therefore results in high dielectric constant and losses.

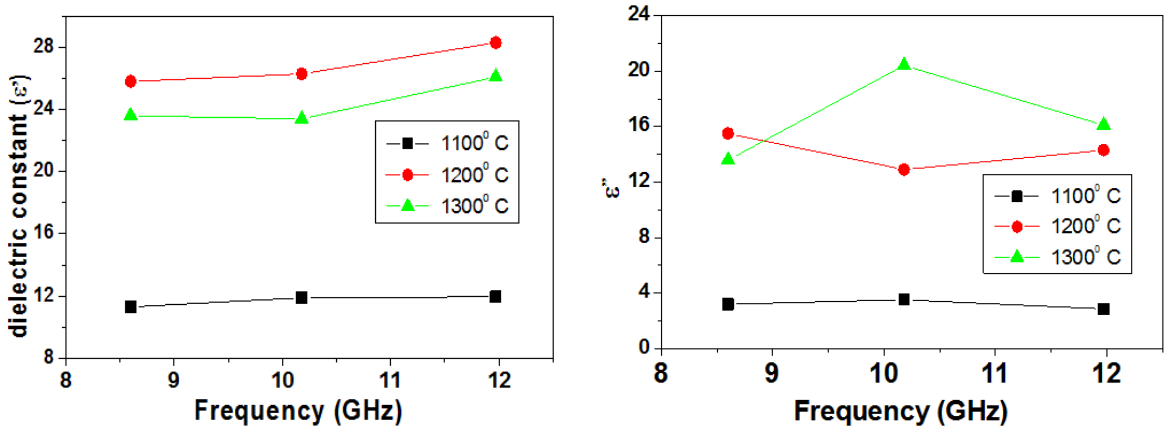

Fig. 3. Permittivity of undoped barium hexaferrite (BaFe12O19) bulk samples measured at X-band frequencies, sintered at different temperatures.

3.2.2 Cation substituted barium Hexaferrite samples

The variation of dielectric constant and loss tangent (tan δ) at RF frequencies for Ba $(CoZr)_xFe_{12-2x}O_{19}$ bulk samples sintered at 1200°C/3h are shown in Fig. 4. The values of dielectric constant and loss are initially high at lower frequencies (below 1 KHz). This is attributed to interfacial dislocation pile-ups, oxygen vacancies, grain boundary defects, etc. in polycrystalline ferrites [34]. With further increase in the frequency, there is a gradual decrease in the values of dielectric constant due to fall in the contribution of orientation polarization in this frequency range. The decrease in dielectric constant and loss tangent as frequency increases and the increase of dielectric constant with increasing sintering temperature (Fig. 4) can be explained by Koop's theory [36], which takes the dielectric structure as an inhomogeneous medium composed of two Maxwell– Wagner type layers. In this model, the dielectric structure is imagined to consist of fairly well-conducting ferrite grains separated by poorly conducting grain boundaries.

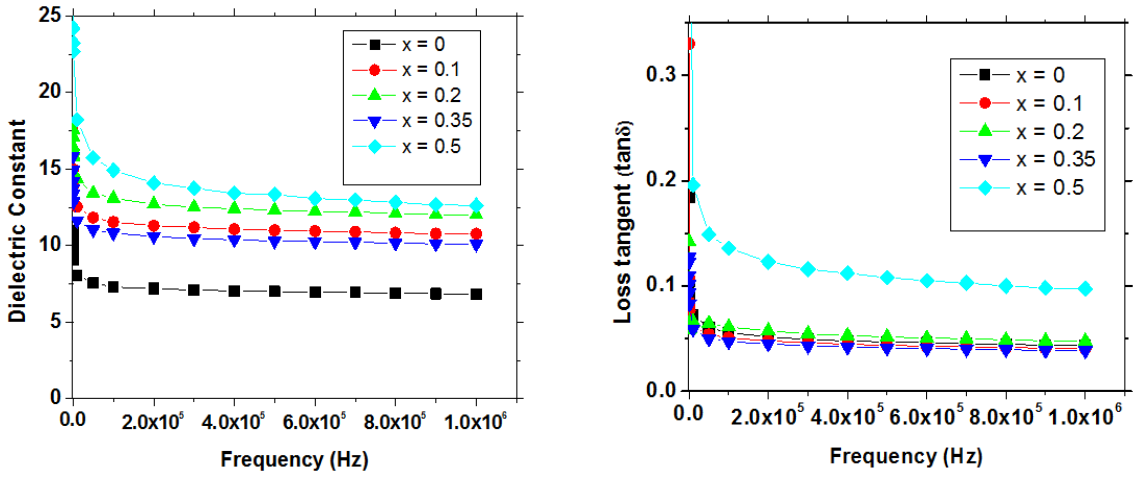

(a) (b)

Fig. 4. Frequency dependence of dielectric constant and loss tangent of Ba(CoZr)xFe12-2xO19 polycrystalline bulk samples

Increase in grain size and density also result in enhanced conductivity and increase in dielectric parameters. The polarization in ferrites has largely been attributed to the presence of Fe^{2+} ions which give rise to heterogeneous spinel structure. It is also visible from the Fig. 4 that Co and Zr substitutions enhance

the dielectric constant and loss factor, possibly more Fe^{2+} ions in crystal lattice sites on substitution. The Fe^{2+} ions being more easily polarizable than Fe^{2+} ions, an increase in Fe^{2+} concentration would result in high electrical conductivity. So samples with low resistivity have higher dielectric constant at low frequencies [39]. Similar behavior in dielectric parameters was also observed in Co-Ti doped barium hexaferrites studied by Haijun et al.[16] .

Compositional dependence of the real and imaginary parts of the complex permittivity measured at 8.6 GHz, and permeability measured at 9.36 GHz are shown in Figs. 5 (a) and (b), respectively, for the $Ba(CoZr)_xFe_{12}$-2xO19 bulk samples sintered at 1200^{0}C / 3h. Permittivity (ε′ and ε′′) decreases upto Co-Zr concentration x = 0.35 and increases on further increase in Co-Zr concentration (x), this may be due to replacement of octahedral Fe^{3+} lattice sites by Co^{2+} and Zr^{4+} ions and again that affects the resistivity and dielectric constant. Co^{2+} cations prefer to occupy the octahedral iron sites (B sites), whereas Zr^{4+} prefers tetrahedral (A sites) iron sites [29]. It is also known that the B sites of a hexagonal ferrite play a dominant role in the phenomenon of electrical conductivity, and the conduction in these ferrites may be due to hopping of electrons in Fe^{3+}+ e ↔ Fe^{2+} at B sites [38]. The substitution of Co^{2+} for Fe^{3+} on the B sites (octahedral sites) acts to reduce Fe^{2+} concentration and also there is hopping between Co^{2+} and Co^{3+}.

Increase in Co and Zr substitution to Fe ions, the number of ferrous and ferric ions at B sites decreases. It seems likely that the concentration of Fe^{2+} on B sites becomes very small whereas the concentration of Fe^{3+} on B site remains high. In terms of a model of electron hopping, the electron exchange is suppressed. Therefore, the dielectric conductivity and consequently the local displacement of electrons in the direction of an external AC electric field (and holes in opposite direction) which determines dielectric polarization in ferrites decrease as Co-Zr substitution increases. Consequently the dielectric constant ε′ and loss tangent decrease as x increases upto x = 0.35. On further increase above this concentration, the excess Co and Zr ions which have to occupy A sites will force the remaining Fe ions at A sites to migrate to B sites. Hopping probabilities between Co^{3+} and Co^{2+} may also become appreciable as the concentration of Co increases. As a result, the dielectric constant increases above this concentration.

Real part of complex permeability (μ') measured at 9.6 GHz, decreases with the increase in the Co-Zr concentration (see Fig. 5(b)), which was expected, because of the substitution of the tetrahedral Fe^{3+} ions by the non-magnetic Zr^{4+} ions, which usually prefer the tetrahedral and bipyamidal lattice sites [29]. Imaginary parts (μ'') also have lower values and it follows the same trend in frequency dependence as μ', which can be seen in Fig. 5(b).

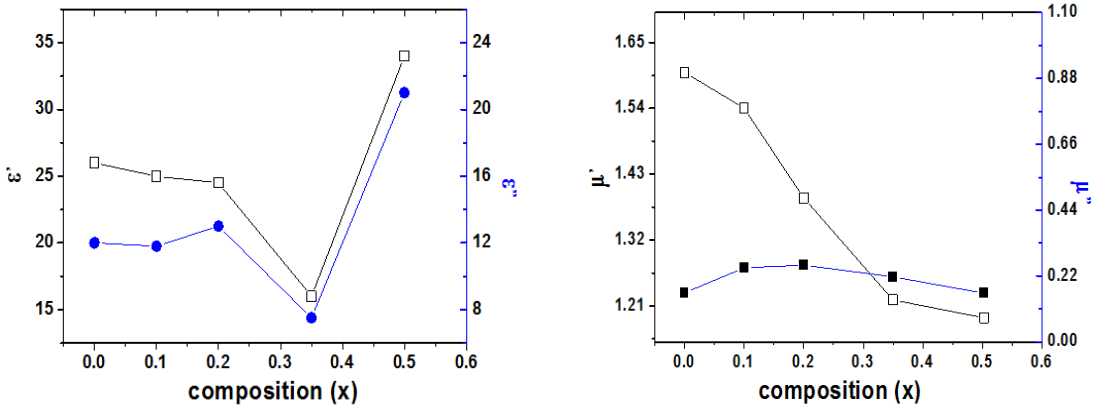

(a) (b)

Fig. 5. Compositional dependence of real and imaginary parts of (a) permittivity (measured at 8.6 GHz), and (b) permeability (measured at 9.36 GHz) of Ba(CoZr)xFe12-2xO19 polycrystalline bulk samples sintered at 1200°C.

3.3. Ferrite–Polymer Composite Thick Films

In the following sections the frequency and temperature dependence of complex permittivity of these ferrite-polymer thick films are discussed.

3.3.1. Dielectric properties at low frequencies

Variation of the dielectric properties of $Ba(CoZr)_xFe_{12-2x}O_{19}$ hexaferrite composite thick films(ferrite to polymer weight ratio was 1:1) with the frequency (50 Hz – 1 MHz) is shown in the Fig. 6. Dielectric constant is nearly constant in the measured frequency range and there was no resonance/dispersion in the measured frequency range upto 1MHz. Permittivity increases with the increase in Co and Zr concentration in ferrite; similar frequency variation of permittivity were observed for bulk hexaferrite samples (see Fig. 5). The polycrystalline ferrite consists of grain and grain boundaries. Orientation polarization is dominant in ferrite-polymer composites [40]. This orientational polarization is the result of the process of electron transfer between ferrous (Fe^{2+}) and ferric (Fe^{3+}) ions [41]. Further, the dielectric losses in the measured frequency range (Fig. 6(b)) are quite low as compared to corresponding bulk ferrites. These properties may be good for device applications, where low losses are desired.

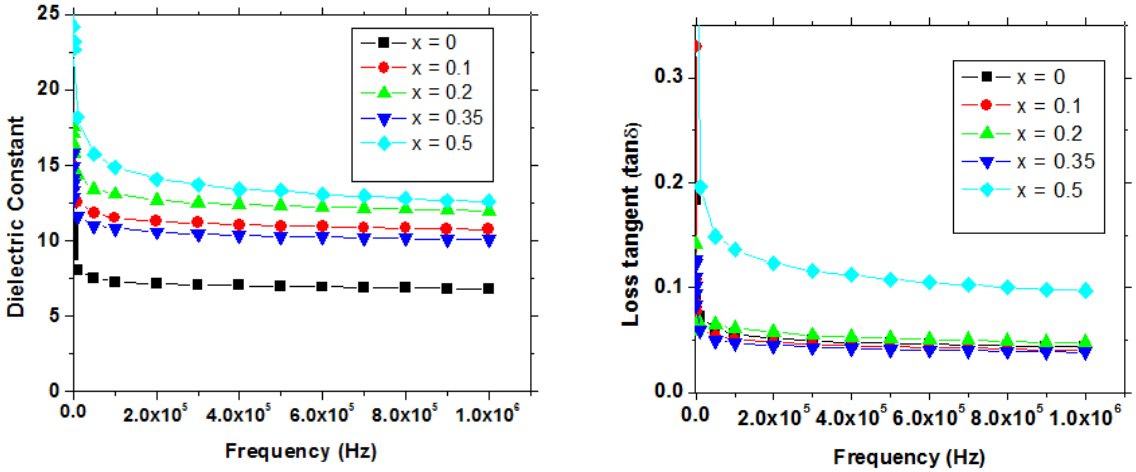

Fig. 6. Frequency dependence of dielectric parameters for the Ba(CoZr)xFe12-2xO19 powders-polymer thick films having a weight ratio of 1:1.

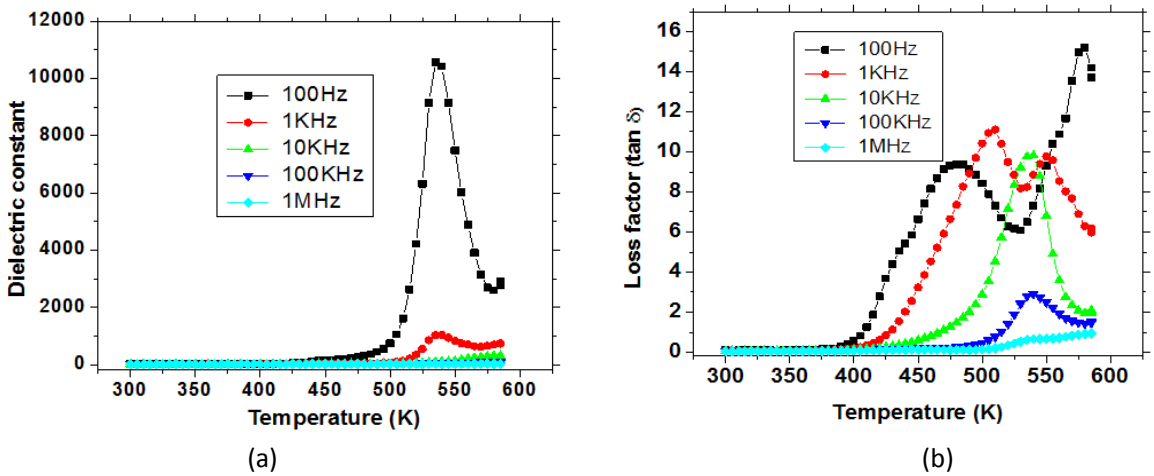

Fig. 7. Variation of dielectric parameters with the temperature for the Ba(CoZr)0.1Fe11.8O19 composite thick film sample (ferrite to polymer weight ratio = 1:1).

Fig. 7 shows the temperature dependence of the dielectric parameters for a representative composite thick film sample ($Ba(CoZr)_{0.1}Fe_{11.8}O_{19}$). Usually the peaks found in dielectric constant - temperature curves may occur either due to the magnetic transition (around Curie temperature) or by electron –hole hopping due to different valence state of Fe^{2+} and Fe^{3+}. But in this case, as can be seen from Fig. 7 (a), the sharp peak is around 250˚C (~523K), which is not the Curie temperature for this ferrite, so it may be due to the electron hopping, this was also observed in other study on Zn-Ti doped barium hexaferrite bulk samples [12]. Also the effects of grain boundaries and the filler polymer can be seen in the broad anomalies around 450K in temperature dependence of dielectric parameters (ε′,ε′′ and tanδ), the peaks related to grains usually appears at higher temperatures. In addition, these peaks showed pronounced frequency dispersion, with the maximum shifting to higher temperature with increasing frequency, which is observed in other ferrite systems as well [12, 33, 35]. The utility temperature of these ferrites may be below those peaks, so the polymer composite films can be utilized at least upto 250°C. The losses are also very low upto the temperatures around 350°C, and dielectric constant as well as loss have lower values at higher frequency (~ 1 MHz).

The dependence of ferrite filling factor on real and imaginary parts of the complex permittivity measured (by cavity perturbation method) at 8.6 GHz for Ba $(CoZr)_{0.5}Fe_{11}O_{19}$-polymer thick film samples is shown in Fig. 8. The values of the dielectric parameters increase with the increase in the fraction of ferrites in the polymer matrix, which is expected due to higher values of dielectric parameters for the hexaferrite (ε' ~ 20) as compared to the polymer (ε' ~ 2). Those values are important for tailoring the electromagnetic parameters for X-band absorbers, because one can choose the optimum compositions which satisfy the condition on the values of ε and μ (ε = μ, for best microwave absorption results).

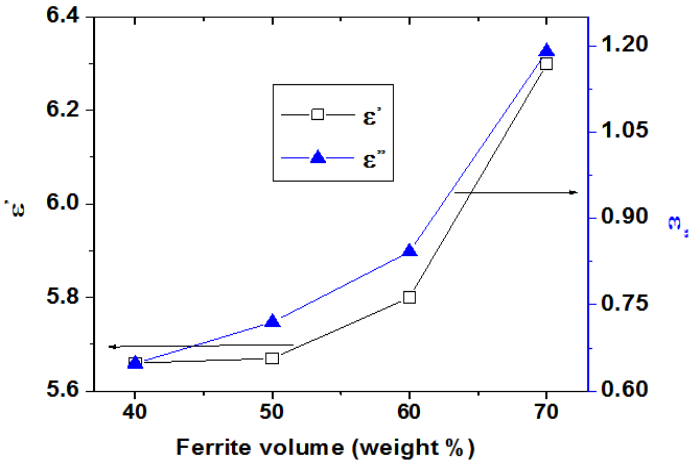

Fig. 8. Dependence of dielectric parameters (measured at 8.6 GHz) on ferrite filling factor in polymer for the Ba(CoZr)0.5Fe11O19-polymer thick film samples.

The variation of the real and imaginary parts of the complex permittivity at microwave frequencies for the Ba $(CoZr)_xFe_{12-2x}O_{19}$ –polymer thick film samples are shown in Fig. 9. These are measured at 3 resonant frequencies due to limitation of the measurement method [26, 27], but we can see that dielectric constant is nearly constant in the measured frequency range of X-band; losses also don't show any remarkable change in this range. This is because these microwave frequencies are too high for orientations polarization which was responsible for fall in ε' with frequency in low frequency region. However, from these figures we can see that the values of real and imaginary parts of complex permittivity are higher for Co-Zr substituted compositions and do not show any frequency resonance or dispersion in this frequency range.

Thus from the frequency dependent measurements on complex permittivity, one can infer that the ferrite-composite thick films do not show any dispersion in dielectric parameters measured either in low frequency region (50 Hz - 1 MHz) or in X-band microwave frequency ranges.

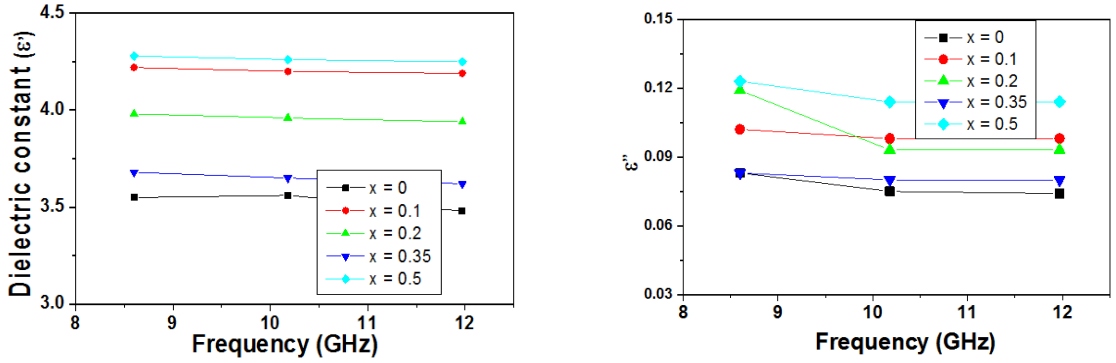

(a) (b)

Fig. 9. Variation of the dielectric parameters with the X-band frequencies for the Ba(CoZr)xFe12-2xO19 – polymer thick film samples.

4. Conclusions

Polycrystalline samples of $Ba(CoZr)_xFe_{12-2x}O_{19}$ ferrites have been prepared by the citrate precursor method, and their composite thick films were screen printed after mixing the ferrite powder with polymer epoxy resin (EPG280). Grain sizes increase on enhancing the sintering temperature, although the grains are smaller as compared to those samples prepared by the conventional ceramic method. Increase in sintering temperatures as well as the CoZr substitution result in increase in the dielectric parameters both at RF and microwave frequencies. The dielectric parameters at both RF and microwave frequencies were measured for thick films, and found to be lower as compared to corresponding bulk materials. Permeability of these samples, measured at X-band frequencies by cavity perturbation technique, were found to be decreasing on Co-Zr substitution, because of substitution of magnetic Fe ions by nonmagnetic Zr ions. However the complex permittivity don't show remarkable change within X-band frequency range because these microwave frequencies are too high for orientation polarization which was responsible for fall in ε' with frequency in low frequency region. The temperature dependence of dielectric properties of these ferrite-composite thick films shows that these can be useful without degradation for applications upto a temperature of 200°C.

Acknowledgements

The experimental work was done in IIT Delhi. Authors thanks Prof. Subhash Kashyap, Physics Department, IIT Delhi for fruitful discussions.

References

[1] Batlle, X., Obradors, X., Rodriguez-Carvajal, J. et al. (1991). Cation distribution and intrinsic magnetic properties of Co-Ti-doped M-type barium ferrite. *J. Appl. Phys. 70*, 1614-1623.

[2] Kreisel, J., Vincent, H., Tasset, F., & Wolfers, P. (2000). The magnetic anisotropy change of $BaFe_{12-2x}Ir_xCo_xO_{19}$: A single-crystal neutron diffraction study of the accompanying atomic and magnetic structures. *J. Magn. Magn. Mater, 213*, 262-270.

[3] Zhou, X. Z., Morrish, A. H., Hong, Y. K., & Li. Z. W. (1991). Site preference for Co^{2+} and Ti^{4+} in Co-Ti substituted barium ferrite. *IEEE Trans. Magn. 27*, 4654-4656.

[4] Kojima, H. (1982). *Fundamental Properties of Hexagonal Ferrites: Ferromagnetic Materials*, Wohlfarth E P (Eds.), New York, North-Holland, 305.

[5] Meshram, M. R., Agrawal, N. K., Sinha, B., & Mishra**,** P. S. (2004). *J. Magn. Magn. Mater, 271,* 207.

[6] Thompson, G. K. and Evans, B. J. (1993). The structure-property relationships in M-type hexaferrites: Hyperfine interactions and bulk magnetic properties*. J. Appl. Phys., 73(10)*, 6295-6297.

[7] Kimura, T., Lawes, G., & Ramirez, A., P. (2005). Electric polarization rotation in a hexaferrite with long-wavelength magnetic structures. *Phys. Rev. Lett. 94*, 137201.

[8] Kitagawa, Y., Hiraoka. Y., Honda, T., Ishikura, T., Nakamura, H., & Kimura, T. (2010). Low-field magnetoelectric effect at room temperature. *Nat. Mater. 9*, 797-802.

[9] Sharbati, A., Choopani, S., Ghasemi, A., Amri, I. A., Machado, C. F. C., & Paesano Jr., A. (2011). *Digest Journal of Nanomaterials and Biostructures, 6 (1)*, 187.

[10] Ozgur, U., Alivov, Y., & Morkoc, H. A. (2009). Microwave ferrites. *J. Mater. Sci: Mater Electron, 20(9)*, 789-834.

[11] Pullar, R. C., Appleton, S. G., & Bhattacharya, A. K. (1998). The manufacture, characterisation and microwave properties of aligned M ferrite fibres*. J. Magn. Magn. Mater. 186*, 326-332.

[12] Dube, C. L., Kashyap, S. C., Pandya, D. K. & Dube, D. C. (2009). Dieletric and magnetic properties of Zn-Ti substituted M-type barium hexaferrite. *Phys. Status Solidi A, 206 (11)*, 2627-2631.

[13] Angeles, A. G., Suarez, G. M., Gruskova, A., Slama, J., Lipka, J., & Papanova, M. (2005). Magnetic studies of Zn–Ti-substituted barium hexaferrites prepared by mechanical milling. *Mater. Lett. 59*, 26-31.

[14] Ghasemi, A., Hossienpour, A., Morisako, A., Saatchi, A., & Salehi, M. (2006). Electromagnetic properties and microwave absorption characteristics of doped barium hexaferrite. *J. Magn. Magn. Mater. 302*, 429-435.

[15] Haijun, Z, Zhichao, L., Chengliang, M., Xi, Y., Liangying, Z., & Mingzhong, W. (2002). Complex permittivity, permeability, and microwave absorption of Zn-and Ti-substituted barium ferrite by citrate sol–gel process, *Mater. Sci. Eng. B 96*, 289-295.

[16] Haijun, Z, Zhichao, L., Chengliang, M., Xi, Y., Liangying, Z., & Mingzhong, W. (2003). Preparation and microwave properties of Co-and Ti-doped barium ferrite by citrate sol–gel process, *Mater. Chem. Phys.*, *80*, 129-134.

[17] Wartewig, P., Krause, M. K., Esquinazi, P., et al. (1999). Magnetic properties of Zn-and Ti-substitued barium hexaferitte. *J. Magn. Magn. Mater. 192***,** 83-99.

[18] Singh, P., Babbar, V. K., Razdan, A., et al. (1999). Complex permeability and permittivity, and microwave absorption studies of Ca $(CoTi)_x Fe_{12-2x} O_{19}$ hexaferrite composites in X-band microwave frequencies. *Mater. Sci. Eng. B 67*, 132-138.

[19] Liu, X., Wang, J., Gan, L. M., & Ng, S. C. (1999). Improving the magnetic properties of hydrothermally synthesized barium ferrite. *J. Magn. Magn. Mater.*, *195*, 452

[20] Mendoza-Suarez, G., Matutes-Aquino, J. A., Escalante-García, J. I., Mancha-Molinar, H., Ríos-Jara, D., & Johal, K. K. (2001). Magnetic properties and microstructure of Ba-ferrite powders prepared by ball milling. *J. Magn. Magn. Mater., 223(1)*, 55-62.

[21] Yu, H. F., & Huang, K. C. (2003), *J. Magn. Magn. Mater.*, *260*, 455.

[22] Janasi, S. R., Emura, M., Landgraf, F. J. G., & Rodrigues, D. (2002). The effects of synthesis variables on the magnetic properties of coprecipitated barium ferrite powders. *J. Magn. Magn. Mater.*, *238*, 168-172.

[23] Wei, F., Lu, M. & Yang, Z. (1999). The temperature dependence of magnetic properties of Zn–Ti substituted Ba-ferrite particles for magnetic recording. *J. Magn. Magn. Mater.*, *191,* 249-253.

[24] Harris, V. G. *et al.*, (2009). Recent advances in processing and applications of microwave ferrites, *J. Magn. Magn. Mater., 321(14)*, 2035-2047.

[25] Li, Z. W., Chen, L., & Ong, C. K. (2002). Studies of static and high-frequency magnetic properties for M-type ferrite $BaFe_{12-2x}Co_xZr_xO_{19}$. *J. Appl. Phys. 92 (7)*, 3902-3907.

[26] Dimri, M. C., Stern, R., Kashyap, S. C., Bhatti, K. P., & Dube, D. C. (2009). Magnetic and dielectric properties of pure and doped barium hexaferrite nanoparticles at microwave frequencies. *Phys. Status Solidi A, 206 (2)*, 270-275.

[27] Verma, A., Saxena, A. K., & Dube, D. C. (2003). Microwave permittivity and permeability of ferrite–polymer thick films. *J. Magn. Magn. Mater., 263,* 228-234.

[28] (2005). CRC Handbook of Chemistry and Physics. (86th ed.), David R. Lide (Eds.), CRC Press, Taylor and Francis, 12, 12 .

[29] Suarez, G. M., Rivas-Vazquez, L. P., Corral-Huacuz, J. C., Fuentes, A. F., & Escalante-Gacia, J. I. (2003). Magnetic Properties and Microstructure of $BaFe_{11.6-2x}$- $Ti_xM_xO_{19}$ (M = Co, Zn, Sn) Compounds, *Physica B, 339*, 110-118.

[30] Iqbal, M. J., Ashiq, M. N., & Gomez, P. H. (2009). Effect of doping of Zr–Zn binary mixtures on structural, electrical and magnetic properties of Sr-hexaferrite nanoparticles. *J. Alloys and Compounds, 478*, 736.

[31] Cullity, B. D. (1978). Elements of X-ray Diffraction. Prentice-Hall.

[32] Dimri, M. C., Kashyap, S. C. & Dube, D. C. (2004). Electrical and magnetic properties of barium hexaferrite nanoparticles prepared by citrate precursor method. *Ceramics International 30*, 1623-1626.

[33] Dimri, M. C., Kashyap, S. C., Verma, A., Dube, D. C., Thakur, O. P., & Prakash, C. (2006). Structural, dielectric and magnetic properties of NiCuZn ferrite grown by citrate precursor method. *Materials Science and Engg. B, 133,* 42-48.

[34] Maxwell, J. C. (1973). *Electricity and Magnetism*. *1*, New York: Oxford University Press, 828.

[35] El, H. M. A. (1999). Dielectric behaviour in Mg–Zn ferrites. *J. Magn. Magn. Mater. 192*, 305-313.

[36] Koops, C. (1951). On the dispersion of resistivity and dielectric constant of some semiconductors at audiofrequencies. *Phys. Rev. 83*, 121.

[37] Smit, J. & Wijn, H. P. J. (1959). *Ferrites. 232*. The Netherlands: Philips Technical Library, Eindhoven.

[38] Purushotham, Y., Reddy, P. V. (1996). Charge transport and conduction mechanism of some substituted strontium W-type hexagonal ferrites. *Inter. J. Moder. Phys. B 10 (3)*, 319.

[39] Brockman, F. G., Dowling, P. H., & Steneck, W. G. (1949). *Phys. Rev.75*, 1440.

[40] Jacob, J., Chia, L. H. L., & Boey, F. C. Y. (1995). *J. Mater. Sc. 30,* 5231.

[41] Abdullah, M. H., & Yusoff, A. N. (1997). Frequency dependence of the complex impedances and dielectric behavior of some Mg-Zn ferrites. *J. Mater. Sc. 32*, 5817-5823.

Mukesh C. Dimri was born in Chamoli, Uttarakhand, India in 1976. He finished M.Sc. degree in physics from HNB Garhwal University, Uttarakhand, India, in 1998. He received his M.Tech. and Ph.D. degree from the Indian Institute of Technology (IIT), Delhi, India, in 2002 and 2007, respectively. Dr. Mukesh C. Dimri is presently working as an assistant professor in Physics and Material Science department, Jaypee University Anoopshahr, UP, India. His research interests are multiferroic, magnetic and spintronic materials, microwave ferrites in nano-structured and bulk form, nanomagnetism, ceramics, composites, multifunctional oxides and thin films.

Dinesh C. Dube received the Ph.D. degree in physics from Delhi University, Delhi, India, in 1970. He has worked in IIT Delhi as Professor of Physics till 2005. He is currently a Professor in the Electrical and Electronics Department, ITM University Gurgaon. His major research interests are high-frequency/ microwave characterization of dielectric, magnetic and ferroelectric materials in thin film as well as in bulk form. Currently, he is working on microwave processing of advanced materials and multifunctional materials.